Green Chemistry

ROYAL SOCIETY OF CHEMISTRY

PAPER

View Article Online
View Journal

Check for updates

Cite this: DOI: 10.1039/c9gc03504d

Smart and sustainable design of latent catalyst-containing benzoxazine-bio-resins and application studies†

Kan Zhang, *[a] Yuqi Liu,[a] Mengchao Han[a] and Pablo Froimowicz*[b]

Received 10th October 2019,
Accepted 8th January 2020

DOI: 10.1039/c9gc03504d

rsc.li/greenchem

A straightforward synthetic approach to incorporate a hydrogen-bonding motif as part of a fully bio-based benzoxazine monomer (**NAR-fa**) is developed, leading to the first latent catalyst-containing thermosetting resin derived from natural renewable resources. The acronym is derived from the phenol (naringenin) and amine (furfurylamine) used in the synthesis. Interestingly, the newly developed benzoxazine resin exhibits a long shelf life in spite of possessing the lowest polymerization temperature reported hitherto for pure benzoxazines, 166 °C. The hydrogen-bonding motif is identified as an important design feature for studying the thermal behavior of the resin. All most common thermal and fire related properties, such as the glass transition temperature (T_g), temperature at which the weight loss is 5 and 10% (T_{d5} and T_{d10}), char yield (Y_c), limiting oxygen index (LOI), heat release capacity (HRC), and total heat released (THR), were far superior to those of typical polybenzoxazines. As a natural consequence of these great characteristics, **NAR-fa** was applied in small amounts (5 mol%) as an initiator and a property modifier of other petroleum-based and natural renewable resourced benzoxazine-based systems. The thermal properties of the resulting copolymeric thermosets were maintained or slightly enhanced, while those related to fire improved by about 38 and 51% for THR and HRC, respectively. These results highlight the utility of the latent catalyst-containing resin design derived from natural renewable resources in the preparation of high-performance resins and thermosets.

Introduction

Fast development in the microelectronic and aerospace industries increasingly requires the novel design of lightweight polymeric materials with outstanding chemical, thermal and mechanical performances.[1] Polybenzoxazine thermosets,[2–5] a relatively new type of polymer, have constantly been drawing particularly strong interest from both industrial applications and academic investigations due to their excellent features, such as a catalyst-free process and near-zero shrinkage during polymerization,[6–8] high thermal resistance,[9,10] low dielectric constant,[11,12] low surface free energy and a very flexible macromolecular design capability.[13,14] Polybenzoxazines can straightforwardly be obtained by the ring-opening polymerization of 1,3-benzoxazine monomers upon heating (Fig. 1a).[3] The relatively stable six-membered heterocyclic oxazine ring is responsible for the long shelf life of benzoxazine resins at room temperature and even in humid environments. However, the high stability of these resins also leads to difficulties in the synthesis and fabrication of polybenzoxazines and polybenzoxazine-based composite materials. For instance, the typical polymerization temperature range for benzoxazine resins exhibiting their exotherm maxima between 220 and 280 °C spans from 160 to 220 °C.[4] Unfortunately, this temperature range is still considered as too high, especially when compared to the usual processing temperatures that are used to produce thermoplastic based composites. Therefore, a reduction in the polymerization temperature of benzoxazine resins is highly desirable for industrial applications.

Adding an initiator and/or catalyst to the benzoxazine resins is an effective approach to decrease the polymerization temperature. In this sense, various catalysts and initiators, such as amines,[15] phenols,[16] carboxylic acids,[17] and many other cationic species[18] have been mixed with benzoxazines to accelerate their polymerization rate. However, most of these studied initiators and/or catalysts show poor solubility or mis-

[a]Research School of Polymeric Materials, School of Materials Science and Engineering, Jiangsu University, Zhenjiang, Jiangsu 212013, P. R. China. E-mail: zhangkan@ujs.edu.cn
[b]Design and Chemistry of Macromolecules Group, Institute of Technology in Polymers and Nanotechnology (ITPN), UBA-CONICET, FADU, University of Buenos Aires, Pabellón III, subsuelo, Ciudad Universitaria (C1428EGA), Buenos Aires, Argentina. E-mail: pxf106@case.edu

†Electronic supplementary information (ESI) available. See DOI: 10.1039/c9gc03504d

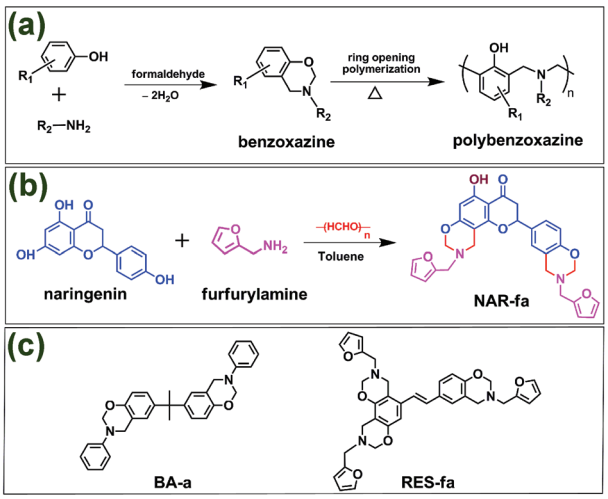

Fig. 1 (a) A general approach for synthesizing benzoxazine resin and its conversion to polybenzoxazine *via* ring-opening polymerization. (b) Synthesis of fully bio-based benzoxazine monomer (**NAR-fa**). (c) Chemical structures of BA-a and RES-fa.

cibility with the benzoxazine systems, and in those cases the good shelf life of the benzoxazine resins is understandably greatly reduced. Alternatively, some catalytically active functionalities, such as hydroxyethyl[19] and phenolic hydroxyl[20,21] have been incorporated into the chemical structure of the benzoxazine itself. Although the active groups enhance the polymerization rate, shortening of the shelf life must be overcome since the catalytically active group disrupts the natural stability of benzoxazine resins. In this regard, a few built-in latent catalyst-containing benzoxazines have also been cleverly developed,[22,23] in which an intramolecular hydrogen-bonding motif seems to offer the needed stable form, in other words the latent or inactive state of the catalyst. This intramolecular hydrogen-bonding motif is still possible to break only upon the application of an external stimulus such as heating, thus forming the very reactive phenolic –OH (active form of the catalyst) able to catalyze the polymerization reaction at much lower temperatures than usual. Thus, a clever exploitation of an intramolecular hydrogen-bonding motif within the chemical structure of the resin results in a highly effective approach to enhance the shelf life of both epoxy and naphthoxazine resins.[22,23]

Unavoidably, the practical application of benzoxazine resins, especially at the industrial scale, is facing the same challenges as most other commercialized polymeric materials in terms of availability of their raw materials. This situation is even worse for those raw materials coming from nonrenewable resources, *e.g.* from petrochemistry. The massive application areas of petroleum-based polymers have generated potential long-term threat and waste accumulation, resulting in environmental pollution.[24] The replaceability of petroleum-based raw materials by natural renewable resources for synthesizing new polymers is attracting great interest from academia as well as industry. These recent efforts invested in developing bio-based thermosets by polymerizing partially or even fully bio-based benzoxazines have paid off by using alternative phenolic and amine compounds from natural renewable resources, especially coming from biomass.[25–30]

In this study, we report a novel fully bio-based benzoxazine (**NAR-fa**) (Fig. 1b), which presents an intramolecular hydrogen-bonding motif formed between a phenolic hydroxyl group and the oxygen atom of a carbonyl. The phenolic compound used, naringenin, is a natural renewable raw material abundant in different fruits, such as grapefruit,[31] sour orange,[32] and tart cherries.[33] The extraction method and content vary depending on the fruit.[32,33] It is worth mentioning that naringenin is demonstrated to be useful for the synthesis of benzoxazine resins for the first time in this work. The amine used to complement the synthesis is furfurylamine, obtained from furfural, which was recognized as a top 10 value-added bio-based chemical by the US Department of Energy.[34] As mentioned in the two previous paragraphs, there are studies reporting on the synthesis of bio-based benzoxazines and on built-in latent catalyst-containing benzoxazines. However, there is no report on a built-in latent catalyst-containing benzoxazine synthesized using bio-based resources. It is in this context that we frame the importance of our results, since this is the very first work reporting the synthesis of a latent catalyst-containing benzoxazine substantially derived from natural renewable resources. The well-designed intramolecular hydrogen-bonding motif present in **NAR-fa** is demonstrated to possess good stability, thus being the latent form of the catalyst-containing benzoxazine, enhancing in consequence the shelf life of the synthesized bio-resin. Once the intramolecular hydrogen-bonding motif is broken upon heating, the phenolic hydrogen becomes more acidic, to the extent of being able to acid catalyze the ring-opening polymerization of benzoxazine thus triggering the reaction at much lower temperatures. Herein, the detailed hydrogen bonding interaction is investigated, as are the thermal and fire related properties of the corresponding polybenzoxazine. Lastly, the use of **NAR-fa** as an initiator as well as a property modifier of other benzoxazine-based systems, such as BA-a (bisphenol-A and aniline-based benzoxazine) and RES-fa (resveratrol and furfurylamine-based benzoxazine) (Fig. 1c), is also presented. The two different successful uses of the bio-based benzoxazine studied in this work represent new approaches to smartly exploit sophisticated benzoxazines for easily enhancing the specific properties of other thermosetting resins or systems.

Experimental

Materials

Naringenin (98%) was obtained from Aladdin Reagent, China. Paraformaldehyde (97%), furfurylamine (99%), acetone, ethyl acetate, hexane and toluene were obtained from Energy Reagent, China. All chemicals were used as received without any further purification. Benzoxazine monomers, BA-a and RES-fa, were synthesized according to previously reported procedures (Scheme S1†).[5,30]

Characterization methods

One dimensional (1D) nuclear magnetic resonance (NMR) spectra of samples in $CDCl_3$ and DMSO-d_6 were recorded on a Bruker AVANCE II 400 MHz NMR spectrometer. 2D ^1H–^1H nuclear Overhauser effect spectroscopy (NOESY) and ^1H–^{13}C heteronuclear multiple quantum coherence (HMQC) were recorded using the same NMR spectrometer. Elemental analysis was conducted on an elementary analyzer (Elementar Vario EL-III). High resolution mass spectrometry (HRMS) was carried out using a Bruker solanX 70 FT-MS mass spectrometer. Fourier transform infrared (FTIR) spectra were recorded using a Nicolet Nexus 670 spectrophotometer. Differential scanning calorimetry (DSC) thermograms were obtained using a NETZSCH DSC apparatus (model 204f1). The temperature ramp rate was 10 °C min^{-1} under a N_2 atmosphere. For the activation energy study, heating rates of 2, 5, 15 and 20 °C min^{-1} were utilized. Thermomechanical analysis (TMA) was carried out using a NETZSCH TMA/402F4 at a heating rate of 5 °C min^{-1}. The coefficient of thermal expansion was calculated in the temperature range from 50 to 250 °C. Dynamic mechanical analysis (DMA) was carried out using a NETZSCH DMA/242E analyzer operating in tension mode, with an amplitude of 10 μm, at the temperature ramp rate of 3 °C min^{-1}, and a frequency of 1 Hz. Thermogravimetric analysis (TGA) was performed using a NETZSCH STA449-C apparatus, from 25 to 850 °C at a heating rate of 10 °C min^{-1} under N_2 and air alternatively. The specific heat release rate (HRR, W g^{-1}) and total heat release (THR, kJ g^{-1}) were obtained using a microscale combustion calorimeter (MCC; Fire Testing Technology), based on the ASTM 7309-2007a standard. The MCC thermogram was recorded from 100 to 750 °C at the heating rate of 1 K s^{-1}, under a stream of N_2 (80 mL min^{-1}); a stream of O_2 (20 mL min^{-1}) was mixed into the anaerobic thermal degradation products under the N_2 gas stream prior to entering the combustion furnace. The temperature of the combustion furnace was set at 900 °C.

Synthesis of 9-(furan-2-ylmethyl)-2-(3-(furan-2-ylmethyl)-3,4-dihydro-2*H*-benzo[*e*][1,3]oxazin-6-yl)-5-hydroxy-2,3,9,10-tetrahydrochromeno[8,7-*e*][1,3]oxazin-4(8*H*)-one (abbreviated as NAR-fa)

Naringenin (1.00 g, 3.70 mmol), furfurylamine (0.72 g, 7.41 mmol), paraformaldehyde (0.47 g, 15.67 mmol) and 30 mL of toluene were added into a 100 mL round-bottom flask equipped with a magnetic stirrer and a condenser. The mixture was stirred at 100 °C for 3 h. After cooling to room temperature, the reaction solution was washed three times with distilled water. The solvent was removed using a rotary evaporator and a white solid was obtained. The product was recrystallized from a solvent mixture of ethyl acetate/hexane (1 : 3), obtaining white needle-like crystals (yield *ca.* 79%).

^1H NMR (400 MHz, $CDCl_3$), ppm: δ = 12.26 (s, 1H, OH), 7.45 (m, 2H, H_f), 7.23 (dd, 1H, H_j), 7.09 (s, 1H, H_k), 6.90 (d, 1H, H_l), 6.38 (m, 2H, H_e), 6.30 (d, 2H, H_d), 6.00 (s, 1H, H_g), 5.30 (dd, 1H, H_i), 4.93 (s, 4H, H_{b1} and H_{b2}), 4.08 (s, 2H, H_{a1}), 3.96 (s, 2H, H_{a2}), 3.95 (s, 2H, H_{c1}), 3.90 (s, 2H, H_{c2}), 3.01–2.77 (m, 2H, H_h).

^{13}C NMR (400 MHz, $CDCl_3$), ppm: δ = 196.17 (C_v), 162.64 (C_u), 160.86 (C_q), 154.55 (C_m), 151.42 (C_o), 151.16 (C_s), 142.70 (C_f), 130.62 (C_p), 126.02 (C_j), 125.83 (C_k), 120.04 (C_r), 116.98 (C_l), 110.29 (C_e), 109.19 (C_d), 102.82 (C_n), 100.21 (C_t), 95.66 (C_g), 82.77 (C_{b1}), 82.01 (C_{b2}), 78.94 (C_i), 49.55 (C_{a1}), 48.39 (C_{a2}), 48.29 (C_1), 44.12 (C_{c2}), 43.29 (C_h).

FT-IR spectra (KBr), cm^{-1}: 1627 (C=O stretching), 1500 (C=C stretching of furfural ring), 1228 (C–O–C antisymmetric stretching), 928 (benzoxazine related band).

Elemental analysis: calculated for $C_{29}H_{26}N_2O_7$: C, 67.70; H, 5.09; N, 5.44. Found: C, 67.59; H, 5.11; N, 5.40.

HRMS-ESI (*m*/*z*): $[M + H]^+$ calculated for $C_{29}H_{27}N_2O_7^+$, 515.1813; found, 515.0093.

Polymerization of benzoxazine monomers

Poly(NAR-fa) was obtained following a stepwise polymerization procedure. Specifically, **NAR-fa** was polymerized in a stainless steel mold in an oven following a four polymerization step procedure. Heating ramps were 10 °C min^{-1} in all cases until reaching the temperature of every polymerization step, which was then isothermally kept at 140, 160, 180 and 200 °C for 1 h each. BA-a and RES-fa were polymerized following the same procedure, thus obtaining poly(BA-a) and poly(RES-fa), respectively.

Synthesis and polymerization of resin blends

BA-a or RES-fa was blended with **NAR-fa** (5 mol%) by gently grinding in a mortar with a pestle in a Teflon mold to form **BA-a/NAR-fa** and **RES-fa/NAR-fa** blends, respectively. These blends were polymerized stepwise, with every step carried out at 140, 160, 180, 200 and 220 °C and kept for 1 h each, thus obtaining **poly(BA-a-*co*-NAR-fa)** and **poly(RES-fa-*co*-NAR-fa)**, respectively.

Results and discussion

Synthesis of NAR-fa

Based on the very flexible molecular design capability of benzoxazine resins, a great number of different benzoxazines have been synthesized, including those coming from natural renewable resources. In most of those cases, the resulting resins presented a single good property or a single advantageous behavior. There are a few reports in which a second functionality has been included into the chemical structure of the benzoxazine resins.[4] However, multi-step reactions, use of protecting groups, and utilization of catalytic systems are indispensable to produce such compounds, as in the case of the synthesis of phenolic hydroxyl group-containing benzoxazines.[20,21] These steps are necessary because the hydroxyl group must be unreactive during the synthesis of the resins, but reactive once the benzoxazine has been already synthesized. Moreover, reaction temperatures must also be carefully controlled since the phenolic –OH is an effective catalyst promoting the ring-

opening of benzoxazines. In this work, we challenge these realities overcoming those synthetic issues but also expressing a revalorization of the natural and renewable resources and, perhaps most importantly, vindicating simplicity. To achieve these goals, we synthesized a novel phenolic hydroxyl group-containing benzoxazine in a straightforward one-pot reaction utilizing naringenin as the phenolic moiety, furfurylamine as the primary amine source, and paraformaldehyde. It is worth mentioning that naringenin has never been utilized in benzoxazine chemistry hitherto.

Naringenin is a flavanone containing three phenolic –OH groups, each of them with a different reactivity. In particular, the one at the 5-position is less chemically reactive due to the intramolecular hydrogen bond that forms with the oxygen of the ketone at the 4-position. We were able to find the right reaction conditions for the other two phenolic –OH groups, at the 7- and 4′-positions, toward their oxazine ring closures, thus obtaining benzoxazine structures, without disrupting the intramolecular hydrogen bond. As shown in Fig. 1a, the newly obtained bio-based benzoxazine monomer, **NAR-fa**, was synthesized under one-pot Mannich reaction conditions. The chemical structure of **NAR-fa** was fully characterized by FT-IR (Fig. S1†), and NMR spectroscopy as well as high-resolution mass spectrometry (HR-MS) and elemental analysis.

In general, the typical ^{1}H and ^{13}C NMR signals for the O–CH_2–N/Ar–CH_2–N and O–CH_2–N/Ar–CH_2–N pairs in benzoxazine compounds consist of two singlets, due to the symmetry of the resins.[4,5] The situation is different in the case of the herein synthesized **NAR-fa**. As can be seen in Fig. 2a, while the proton signals related to the two O–CH_2–N groups are well overlapped at 4.93 ppm, the characteristic ^{1}H NMR resonances associated with the two Ar–CH_2–N groups belonging to each oxazine ring of **NAR-fa** are observed in the spectrum at 4.08 and 3.96 ppm. This result evidences that the two Ar–CH_2–N groups are in magnetically different surroundings. Complementarily, the typical resonances of the two methylene groups belonging to the furfurylamine moieties are observed in the spectrum as two different signals at 3.95 and 3.90 ppm. Again, this result shows that the two methylene groups are in magnetically different surroundings. The combination of these results with the integration ratio of all signals provides evidence that: (a) only one of the possible **NAR-fa** isomers was obtained under the reaction conditions established in this work, and (b) the chemical structure of this isomer is asymmetric.

Once it was established that only one isomeric form of **NAR-fa** was obtained following the herein described synthesis protocol, additional 2D NMR spectroscopic studies were necessary to further confirm the correct configuration of the isomer and to unambiguously assign those methylene groups that are heavily overlapped.[35] A thorough analysis revealed that H_g does not present any NOE interaction (Fig. S2†), strongly suggesting that this proton is at the *ortho*-position with respect to the phenolic –OH. Conversely, if this oxazine ring would have been formed closing the ring at the *ortho*-position with respect to the phenolic –OH, there would have been a proton

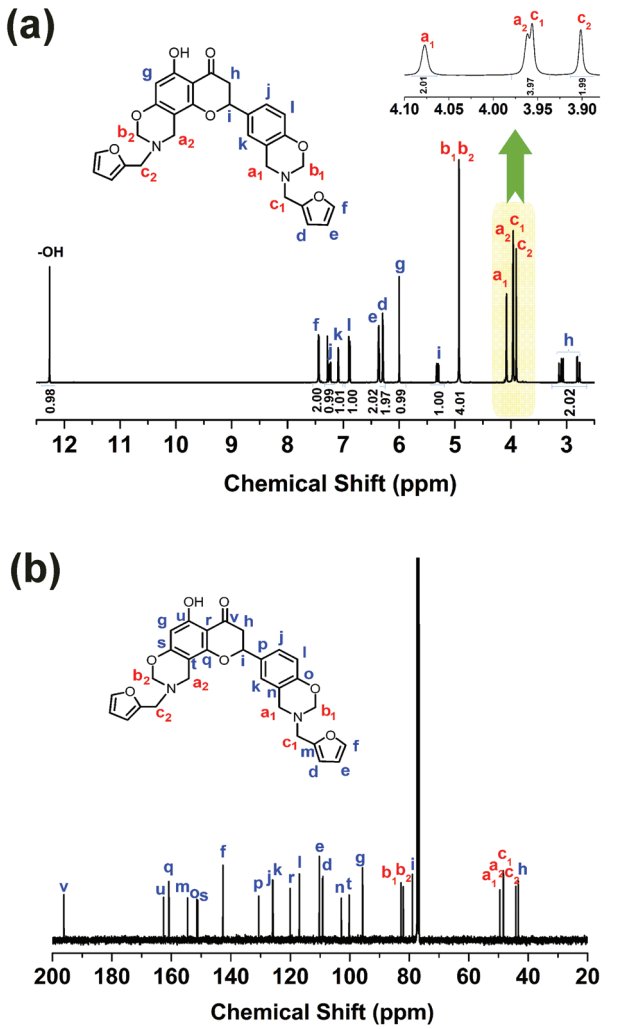

Fig. 2 ^{1}H (a) and ^{13}C (b) NMR spectra of **NAR-fa**, using $CDCl_3$ as the solvent.

at the *para*-position with respect to that same –OH close enough to experience the NOE effect with H_i. However, this interaction is not detected in the 2D ^{1}H–^{1}H NOESY NMR spectrum of **NAR-fa**. Concerning the NOE effect related to the methylene groups, it was observed that H_k presents a strong interaction with H_{a1}, which interacts with H_{b1} and H_{C1}, and the latter with H_d. The complete ^{1}H NMR spectrum elucidation of **NAR-fa** is shown in Fig. 2a. In addition, Fig. 2b shows the ^{13}C NMR spectrum of **NAR-fa**. The carbon resonances assigned in this spectrum were obtained establishing the corresponding correlations from the ^{1}H NMR spectrum into the ^{1}H–^{13}C heteronuclear multiple quantum coherence (HMQC) NMR spectrum (Fig. S3†).

Thermal behavior and polymerization of the benzoxazine monomer NAR-fa

The thermal behavior of **NAR-fa** was studied by DSC and complemented by *in situ* FT-IR spectroscopy. Fig. 3a shows that there are two thermal events in the DSC thermograms of **NAR-**

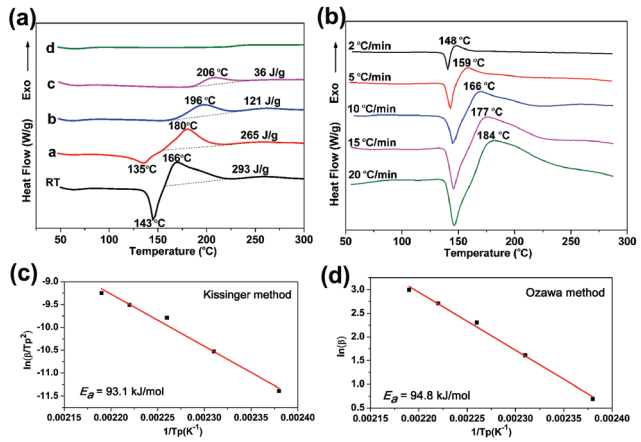

Fig. 3 (a) DSC thermograms of **NAR-fa** after each polymerization step. a: 1 h at 140 °C; b: 1 h at 140 °C + 1 h at 160 °C; c: 1 h at 140 °C + 1 h at 160 °C + 1 h at 180 °C; d: 1 h at 140 °C + 1 h at 160 °C + 1 h at 180 °C + 1 h at 200 °C. (b) DSC thermograms of **NAR-fa** at five different heating rates. Plots generated applying the Kissinger (c) and Ozawa (d) methods to graphically calculate the activation energy for the polymerization reaction of **NAR-fa**.

fa. The first one is an endothermic process, whose minimum is observed at 143 °C, and is assigned to the melting of the naringenin-based benzoxazine crystals. The sharpness of this endotherm provides evidence for the high purity of **NAR-fa**, which was further confirmed by elemental analysis and high resolution mass spectrum. The second thermal event is an exothermic process, whose onset is at 149 °C and its corresponding maximum at 166 °C, and is assigned to the ring-opening polymerization of the benzoxazine monomer.

The extremely low polymerization temperature of **NAR-fa** successfully responds to our chemical design of a built-in latent catalyst-containing benzoxazine. This result exceeded our expectations since we have established a very simple one-pot synthesis procedure, which, to the best of our knowledge, produced the benzoxazine resin with the lowest polymerization temperature among all previously reported benzoxazines, without any addition of catalysts or initiators.[4,5,23,28] The role played by the phenolic –OH facilitating the reduction of the polymerization temperature is crucial and will be discussed in the next section, Intramolecular hydrogen bonding and the latent-catalyzed effect.

Polymerization of the fully bio-based benzoxazine **NAR-fa** was carried out following a convenient four-step procedure. To establish this procedure, it was first necessary to evaluate the reaction efficiency obtained after every single polymerization step. It can be seen in Fig. 3a that the thermogram corresponding to the first polymerization step presents the endothermic peak shifted to a lower temperature (135 °C) while the exothermic one to a higher temperature (180 °C). The shifting of these thermal events accompanied by a decreased heat of polymerization (265 J g^{-1}) compared to the original sample (293 J g^{-1}) clearly suggest that **NAR-fa** has been partially polymerized. The thermogram corresponding to the second polymerization step shows only an exothermic peak, which is further shifted (196 °C) and involves a lower heat of polymerization (121 J g^{-1}) than that of the previous thermogram. This same tendency is observed on the thermogram corresponding to the third polymerization step (maximum at 206 °C and heat of polymerization of 121 J g^{-1}). Finally, the thermogram corresponding to the fourth polymerization step shows that no thermal events are detectable, thus suggesting that NAR-fa is fully polymerized under these conditions. To gain a deeper understanding on the polymerization behavior of **NAR-fa**, the *in situ* FT-IR qualitative analysis was performed (Fig. S4†). The characteristic absorption bands around 1228 cm^{-1} (C–O–C antisymmetric stretching mode) and 928 cm^{-1} (benzoxazine related mode) are used to study the ring-opening polymerization of the oxazine rings belonging to **NAR-fa**. The gradual decrease of these bands as a function of the heat applied in each polymerization step, followed by their complete disappearance after having carried out the fourth thermal treatment, clearly supports the DSC results, where it was observed that **NAR-fa** fully reacted upon heating *via* ring-opening polymerization.

The activation energy (E_a) for the polymerization reaction of **NAR-fa** was investigated on applying the nonisothermal method by DSC at the following heating rates 2, 5, 10, 15 and 20 °C min^{-1}. The corresponding DSC thermograms are shown in Fig. 3b. Herein, the activation energy of the polymerization reaction of **NAR-fa** is simply calculated using the well-known Kissinger and Ozawa theories,[36,37] applying the following equations:

$$\text{Kissinger equation: } \ln\left(\frac{\beta}{T_p^2}\right) = \ln\left(\frac{AR}{E_a}\right) - \frac{E_a}{RT_p} \quad (1)$$

$$\text{modified Ozawa equation: } \ln\beta = -1.052\frac{E_a}{RT_p} + C \quad (2)$$

where β is the constant heating rate and T_p is the maximum value of the exothermic polymerization peak observed on the thermograms obtained by DSC, E_a is the activation energy for polymerization, R is the gas constant, and A is the frequency factor. Thus, the corresponding plots were obtained showing in both cases straight lines when following the two methods, and the E_a values were calculated to be as low as 93.1 (Kissinger) and 94.8 (Ozawa) kJ mol^{-1} (Fig. 3c and d).

As in both cases, following the Kissinger and the modified Ozawa methods, the graphical tendency is linear, a single, or at least a predominant, mechanism is assumed to occur during the polymerization of **NAR-fa**. Importantly, the calculated activation energy for this polymerization resulted to be much lower than those of most reported benzoxazine resins.[38,39] In other words, to the great advantage of the extremely low polymerization temperature, we must also consider that **NAR-fa** is easy to activate toward its polymerization with low energy levels, and no less important the polymerization reaction follows a single mechanism. All these tremendous advantages are mostly due to the existence of the unique built-in latent catalyst-containing benzoxazine monomer. At this

point it must also be highlighted that these advantages are not only for this monomer in itself, but they can smartly be exploited to enhance other systems, such as reducing polymerization temperatures, saving energy, and tailoring properties, as will be exemplified next in a section called Application of **NAR-fa** as an initiator and a property modifier.

Intramolecular hydrogen bonding and the latent-catalyzed effect

As demonstrated in the previous sections, **NAR-fa** polymerizes at lower temperature than any other ordinary benzoxazine without added initiators and/or catalysts.[4,5] A few benzoxazine-like resins containing a phenolic –OH group as part of their chemical structure have been reported to experience an efficient catalytic effect lowering the polymerization temperatures.[16,23] Nevertheless, the magnitude of such an effect has never been as impressive as the one experienced by the herein synthesized naringenin-based benzoxazine, **NAR-fa**. In agreement with the reported data from the literature,[23] the acidity of the phenolic –OH at relatively high temperature seems to be high enough to act as a strong driven force stimulating the observed polymerization at low temperature. However, at moderate to low temperatures the presence of a six-membered-ring hydrogen-bonding system between the phenolic –OH and the oxygen atom of the ketone makes this resin very stable and easy to store. Thus, we developed an interest in understanding the molecular nature of this possible hydrogen bonding system governing these behaviors. To achieve this goal, we designed a series of spectroscopic experiments, whose results are presented in Fig. 4.

The first piece of evidence suggesting the existence of this hydrogen-bonding system came from the very simple 1D ^{1}H NMR spectrum obtained using $CDCl_3$ as the solvent. It is well-known in ^{1}H NMR spectroscopy that the quality and chemical shift of proton signals corresponding to –OH groups, such as the phenolic –OH under study, are strongly influenced by the utilized solvent. Specifically, $CDCl_3$ has the particularity of producing an intermolecular proton–deuterium exchange with the –O*H* of the sample, making sometimes the analyses difficult due to the signal distortion. Even in those cases where the signal can be detected and assigned, integration is rarely acceptable. However, if the mobility of the –O*H* is reduced to such an extent of eliminating the proton–deuterium exchange, then the signal quality is restored. The latter is what occurs when the –O*H* is "trapped" as part of a molecular motif because of its involvement in strong hydrogen-bonding systems. This is what we have identified in the ^{1}H NMR spectrum of the naringenin-based benzoxazine monomer, **NAR-fa**, an extremely well defined singlet with a perfect integration ratio for the –O*H*. A second piece of evidence supporting this hydrogen bond also coming from the same spectrum is the unusually very high chemical shift of the –O*H* signal, observed at 12.26 ppm. This is due to the fact that stronger hydrogen bonds make the involved protons more deshielded, thus inducing downfield chemical shifts (high frequency, higher ppm values). The third piece of evidence using $CDCl_3$ as the solvent was by carrying out the typical concentration-dependent experiments, for which the no variation of the chemical shift of the –O*H* signal while varying the concentration of the **NAR-fa** solutions strongly supports, once again, the existence of the intramolecular six-membered-ring hydrogen-bonding system. This result is presented qualitatively in Fig. 4a and quantitatively in Fig. 4b.

To complement the previous studies, the ^{1}H NMR spectra of **NAR-fa** samples were also investigated using DMSO-d_6 as the solvent (Fig. S5†). The differential solvent shift experiment helps to estimate a relative strength of a given hydrogen bond. It must be mentioned that while DMSO-d_6 is a strong hydrogen-bonding acceptor, $CDCl_3$ is a weak hydrogen-bonding donor and acceptor. The magnitude of the –O*H* signal shifting is calculated as $\Delta\delta = \delta(\text{DMSO-}d_6) - \delta(CDCl_3)$, where the larger the chemical shift difference, the weaker the interaction. In our case, the phenolic –O*H* signal is observed at 12.38 ppm using DMSO-d_6 as the solvent (Fig. 4c), thus obtaining a $\Delta\delta$ of 0.12, which suggests a very strong hydrogen-bonding system. The combination of all previous results permits solidly proposing the chemical structure of **NAR-fa** in both $CDCl_3$ and DMSO-d_6 at room temperature as depicted in Fig. 4d, where the intramolecular hydrogen bonding is denoted in green hashed lines and the six-membered-ring hydrogen-bonding motif inside the orange circle.

As the polymerization of **NAR-fa** is induced by heat, we were clearly interested in verifying the behavior of this hydrogen bond at different temperatures. It was observed that the nicely defined –O*H* signal shifted to higher fields (lower ppm) while broadening, indicating that the intramolecular hydrogen-bonding system was weakening upon heating (Fig. 4c). There should certainly be a temperature at which the hydrogen bond would be weak enough to let the proton go free without being "trapped" any more by the six-membered-ring hydrogen bond. Keeping in consideration that the ring-opening polymerization of benzoxazine resins is acid catalyzed, one can consider that the latent-catalyst can be activated by breaking the hydrogen bonding system upon heating. Therefore, the polymerization of **NAR-fa** is easy to assume as the on/off capability of the intramolecular six-membered-ring hydrogen-bonding system.

The high stability under ambient conditions combined with the high reactivity under polymerization conditions demonstrated by **NAR-fa** evidences its latent-catalyst efficiency thanks to the on/off capability of the intramolecular hydrogen bonding system. Thus, it is assumed that at room temperature the intramolecular hydrogen-bonding system acts as a protecting group having the phenolic proton "trapped" within the six-membered ring, in other words, inactive. Moreover, this stability was further tested by thermally treating **NAR-fa** at 60 °C and even at 100 °C for 1 h. The products of these tests were examined by DSC. The three thermograms, corresponding to the untreated **NAR-fa** and the two thermally treated samples, exhibit the very same profile along the entire temperature range, from 30 to 300 °C (Fig. S6†). This result not only shows the high thermal stability of **NAR-fa**, but also reinforces the existence of the latent-catalyst effect of the naringenin-based resin. There is, however, a certain temperature at which the

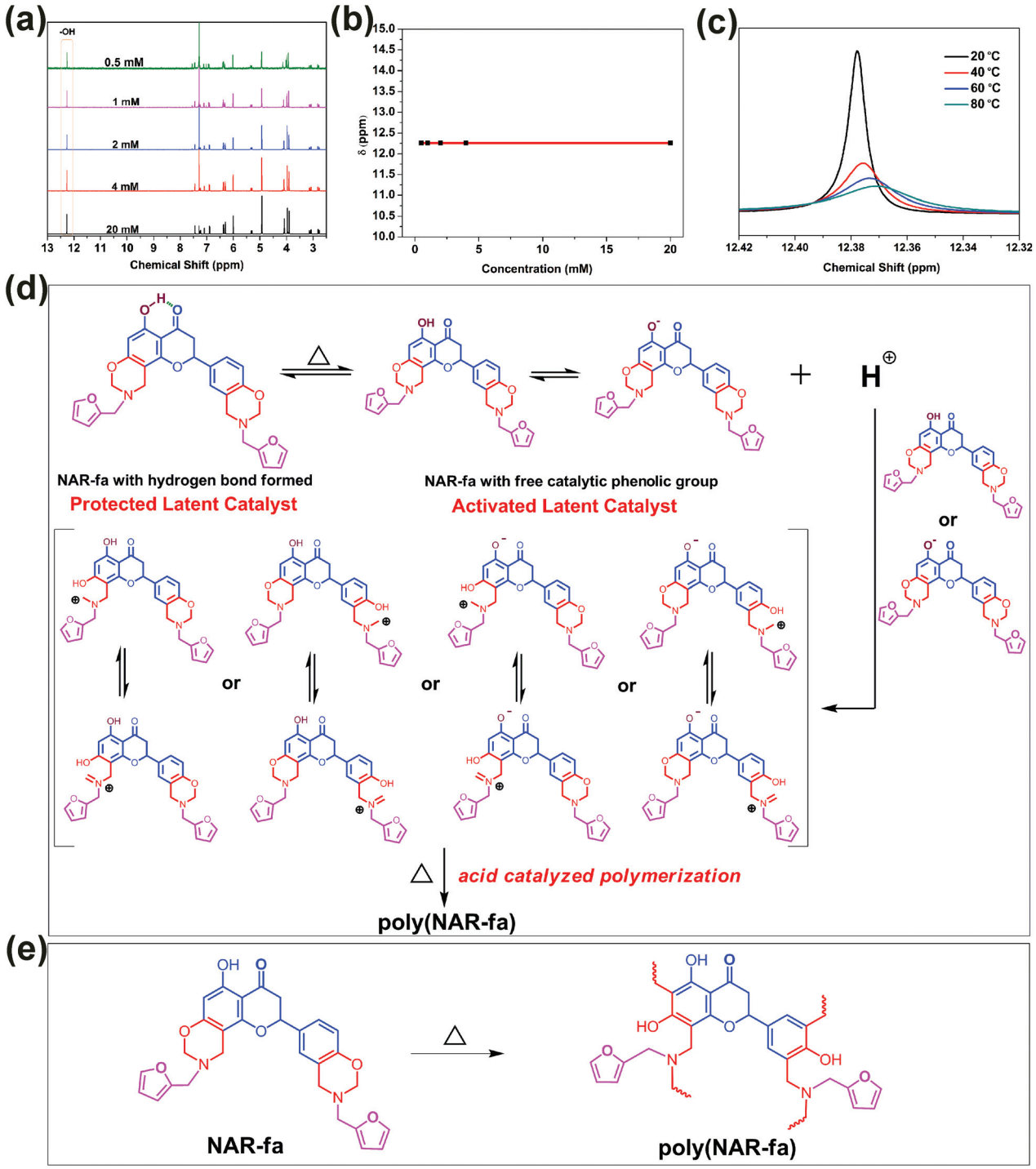

Fig. 4 (a) ^{1}H NMR spectra for **NAR-fa** in $CDCl_3$ at five different concentrations. (b) Result of the concentration-dependent experiments using data extracted from the ^{1}H NMR spectra in $CDCl_3$ for **NAR-fa** at different concentrations. (c) Peak shifting of the phenolic proton of **NAR-fa** in ^{1}H NMR spectra using DMSO-d_6 as the solvent at four different temperatures. (d) Proposed mechanism of the built-in latent catalyst activity and ring-opening polymerization of **NAR-fa**. (e) The chemical structure of the obtained polybenzoxazine (**poly(NAR-fa)**).

six-membered-ring hydrogen-bonding system weakens enough to let the phenolic proton interact with the oxygen and/or nitrogen atoms belonging to the oxazine rings. This process will influence the reactivity of the benzoxazine triggering the polymerization reaction. It is important to highlight that the proposed mechanism presented in Fig. 4d is in full agreement with all considerations already established for the acid catalyzed polymerization of benzoxazines.[8]

An additional interesting result obtained upon spectroscopic studies is that **NAR-fa** is highly stable under ambient

conditions, thus offering easy approaches to store it with a demonstrated long shelf-life. For instance, this resin has also been proven to be very stable even in solution. Fig. S7 and S8† show the full ^{1}H NMR spectra of **NAR-fa** in both $CDCl_3$ and DMSO-d_6 for samples freshly prepared and analyzed as well as those recorded after three months of storage. No changes are seen in the corresponding spectra, except for a slight moisture increase in the sample prepared using DMSO-d_6 as the solvent.

Thermal properties of the polybenzoxazine poly(NAR-fa). The thermomechanical properties of **poly(NAR-fa)** (Fig. 4e) were investigated by both thermomechanical and dynamic mechanical analyses, TMA and DMA, respectively. Fig. S9† shows the TMA curve obtained for the **poly(NAR-fa)** film. The coefficient of thermal expansion (CTE) was calculated from the TMA experiments and found to be 54.7 ppm °C^{-1}, which compares positively to the reported CTE of the bisphenol A epoxy resin of 70 ppm °C^{-1}.[40] TMA also allowed the determination of T_g, 278 °C, of this thermoset. Notably, **poly(NAR-fa)** shows a much higher T_g value when compared to most other reported benzoxazine resins polymerized at similar or relatively higher polymerization temperatures.[4,5] This value was corroborated by DMA, considering the temperature at the peak maximum of tan δ as a function of the temperature as the T_g. Thus, it can be seen in Fig. 5a that **poly(NAR-fa)** exhibits a T_g value of 286 °C, which is consistent with that determined by TMA.

The thermal stability of **poly(NAR-fa)** was quantitatively evaluated by thermogravimetric analysis (TGA) (Fig. S10†). The temperature at which a weight loss corresponding to 5% is measured is defined as T_{d5}, while that at 10% is T_{d10}. Usually, these two values are reported in conjunction with the char yield (Y_c), which is defined as the residual weight percentage measured at 800 °C. The results summarized in Table S1† show the high stability of **poly(NAR-fa)**, which is fairly comparable to most of the classical benzoxazines based on nonrenewable resources.[4,5] If we only consider natural renewable resource-based benzoxazines instead, then the thermal stability of **poly(NAR-fa)** is among the highest simultaneously considering its T_{d5}, T_{d10}, and Y_c.[28] As a consequence of this result, we developed as well an interest in evaluating its thermal stability in air. As seen in Table S1†, the T_{d5} and T_{d10} values obtained in air are almost identical to those observed under a nitrogen atmosphere, once again evidencing the extraordinary high thermal stability of **poly(NAR-fa)**. It is only after temperatures of about 410 to 415 °C that this stability in air is lost due to thermal combustion.

Notably, the pronounced broadness of the derivative peaks (Fig. S10a†) indicates a slow degradation rate over a wide temperature range, which, in general, is considered as beneficial from a flammability standpoint.[41] In this context, the limiting oxygen index (LOI), defined as the minimum oxygen percentage in an oxygen/nitrogen mixture present in the continuous combustion of polymeric materials, can be used to initially although quantitatively assess the flame-retardant capability of **poly(NAR-fa)**. Thus, the LOI value obtained for poly(RES-fa) applying the van Krevelen equation is as high as 43.1.[42] The real meaning of this value comes to light taking into consideration that there is, on average, 21% oxygen present in atmospheric air, therefore any polymeric material with a LOI value under 21% easily burns in air. LOI values between 21 and 28% are representative for the so-called slow-burning materials. However, if the LOI values are greater than 28%, we are then in the presence of a self-extinguishing material, which will cease burning once removed from the ignition source.[43]

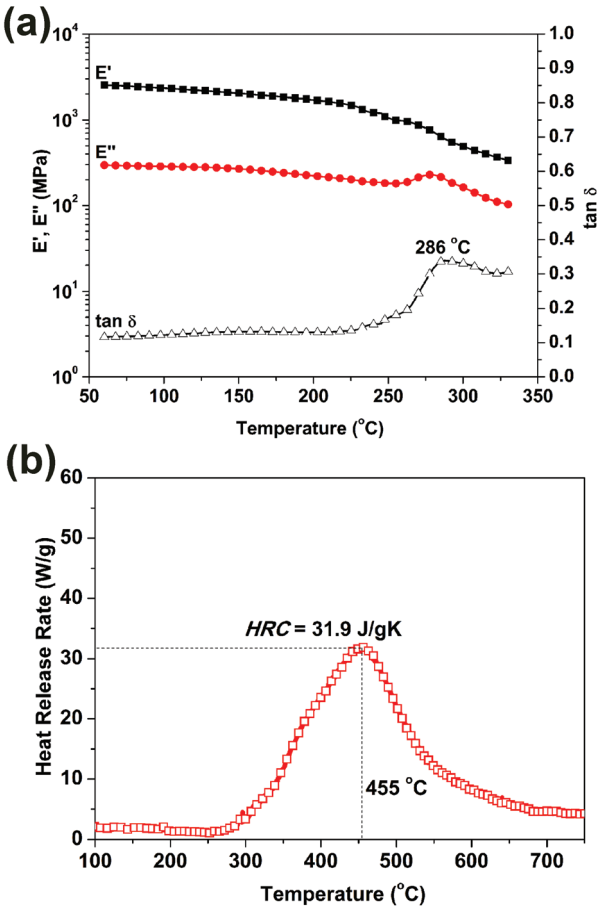

Fig. 5 (a) Dynamic mechanical analysis of **poly(NAR-fa)**. (b) Microscale combustion calorimetric (MCC) analysis of **poly(NAR-fa)**. Plots of the heat release rate as a function of temperature.

Microscale combustion calorimetry (MCC) was also carried out to complement the previous result and evaluate other quantitative properties related to the flammability of **poly(NAR-fa)**. Fig. 5b shows the graphics of the heat release rate (HRR) as a function of temperature, where the HRR maximum is observed at 455 °C. Properly using the information contained in Fig. 5b permits the calculation of the heat release capacity (HRC) and total heat released (THR) for **poly(NAR-fa)**. In particular, a HRC and THR of 31.9 J g^{-1} K^{-1} (Fig. 5b) and 6.6 kJ g^{-1} (Fig. S11†), respectively, were calculated. The HRC value for **poly(NAR-fa)** is even much lower than those reported for polybenzoxazines with very low flammability obtained upon the polymerization of *ortho*-amide and *ortho*-imide functional benzoxazine monomers.[44,45] These results show that **poly(NAR-fa)** can indeed be classified as non-ignitable given that its HRC is lower than 100 J g^{-1} K^{-1}.[46]

The combination of all previous results demonstrates the high thermal stability accompanied by a low flammability of the herein fully bio-based polybenzoxazine obtained upon a very low temperature polymerization without any additive of a benzoxazine monomer synthesized only using natural renewable resources as raw materials, naringenin and furfurylamine. This smart design of monomers highly contributes to the generation of a high-performance thermoset, thus making **poly(NAR-fa)** very attractive for applications requiring high thermal stability and fire resistant properties.

Application of NAR-fa as an initiator and a property modifier of other benzoxazine systems. On the basis of the tremendous advantages shown by the benzoxazine resin, **NAR-fa**, and the excellent properties of the resulting thermoset, **poly(NAR-fa)**, great interest immediately emerged in evaluating this novel latent catalyst-containing resin toward its utilization to induce enhanced properties over other more classical benzoxazine systems. This would easily help to expand their possible applications. To achieve this goal, the herein synthesized bio-based resin was specifically studied with regard to its power to influence the polymerization temperature and fire-related properties of the classic thermoset obtained upon the polymerization of benzoxazine BA-a, which is the most applied benzoxazine.[4,5] To make this study extensive to bio-based benzoxazines, the recently reported resin RES-fa[30] was also included in this analysis. Thus, four different thermosets were designed and carefully prepared to compare their behaviors, specifically, two homopolymers poly(BA-a) and poly(RES-fa),

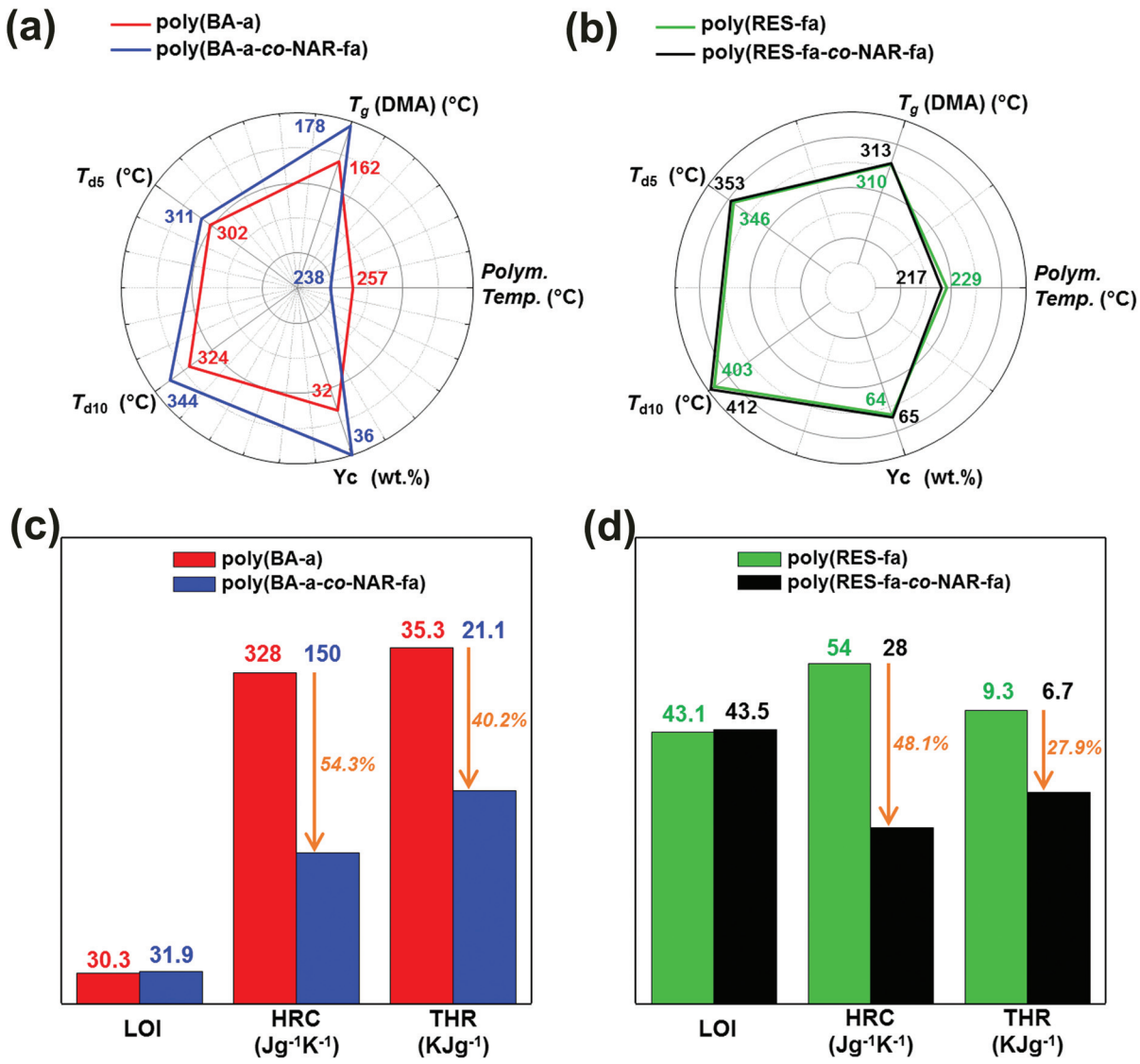

Fig. 6 Thermal and fire related properties of pure poly(BA-a) and poly(RES-fa) homopolymeric thermosets as well as **poly(BA-a-*co*-NAR-fa)** and **poly(RES-fa-*co*-NAR-fa)** copolymeric thermosets. Comparisons of polymerization temperature and thermal stability between poly(BA-a) and **poly(BA-a-*co*-NAR-fa)** (a), and between poly(RES-fa) and **poly(RES-fa-*co*-NAR-fa)** (b). Comparisons of flame retardancy related properties between poly(BA-a) and **poly(BA-a-*co*-NAR-fa)** (c), and between poly(RES-fa) and **poly(RES-fa-*co*-NAR-fa)** (d).

and two copolymers **poly(BA-a-*co*-NAR-fa)** and **poly(BA-a-*co*-NAR-fa)**, both containing 5 mol% of **NAR-fa**. The results are shown in Fig. 6.

As can be seen in Fig. 6a, the polymerization temperature of the copolymers, **poly(BA-a-*co*-NAR-fa)**, is lower than that of the homopolymer, poly(BA-a). This figure also shows that the common thermal properties (T_g, T_{d5}, T_{d10}, and Y_c) of the copolymeric thermoset are always greater in values than those of the homopolymeric thermoset poly(BA-a). These results clearly provide evidence that **NAR-fa** not only is a latent catalyst-containing benzoxazine able to polymerize at low temperatures but it can also be used to lower the polymerization temperatures of other benzoxazines. Moreover, even when used in low content (5 mol%), **NAR-fa** can positively influence the thermal properties of the resulting thermoset. The observed enhancement in each thermal property is interpreted as due to an increment of the crosslinking density of the copolymeric thermoset in comparison to the homopolymeric one, possibly mediated by the reactivity of the phenolic –OH and a few phenoxy groups during the propagation step. Similar behaviors were observed when using **NAR-fa** as an additive to influence the properties of the bio-based RES-fa resin as well as its thermoset. As seen in Fig. 6b, however, the magnitude of these changes is less important than in the previous case. This can be due to the fact that poly(RES-fa) has a naturally higher crosslinking degree than poly(BA-a), thus being less affected by the small amount of **NAR-fa** present in the reactive mixture and in the final product once polymerized.

The fire related properties were also studied to evaluate if this small amount of **NAR-fa** would influence and in what magnitude the natural behavior of other thermosets. Fig. 6c and d show how a 5 mol% of **NAR-fa** into the studied thermosets strongly affects their fire-related properties. Understandably, the LOI values were somehow similar since the Y_c values of the compared thermosets were close. However, a very impressive result is observed in Fig. 6c where an enhancement of about 54.3% and 40.2% is observed for the HRC and THR, respectively, for the thermosets containing a 5 mol% of **NAR-fa** with respect to those not having it. The same results were obtained for the studied bio-based thermoset shown in Fig. 6d, where an enhancement of about 48.1% and 27.9% is observed for the HRC and THR, respectively, for the copolymeric thermosets with respect to the homopolymeric ones.

Conclusions

In summary, a novel latent catalyst-containing bio-based benzoxazine monomer, **NAR-fa**, was smartly designed and successfully synthesized using naringenin, furfurylamine, and formaldehyde as raw materials. **NAR-fa** was shown to readily undergo a thermal activation of its latent-catalytic system, the intramolecular hydrogen bonded –OH, which then efficiently catalyzed the polymerization reaction at a temperature as low as 166 °C without adding any initiator or catalyst to the reaction media. The fully bio-based polybenzoxazine obtained, **poly(NAR-fa)**, exhibited a T_g of 286 °C accompanied by an excellent thermal stability, as reflected by its T_{d5} and T_{d10} values, 361 °C and 404 °C, respectively, in addition to a char yield of 64%. Moreover, **poly(NAR-fa)** was also shown to be a self-extinguishing and non-ignitable material given the low heat release capacity (HRC of 31.9 J g^{-1} K^{-1}) as well as low total heat release (THR of 6.6 kJ g^{-1}). Therefore, the combination between the green raw materials, latent-catalyzed polymerization characteristics, the outstanding thermal properties of this thermoset on its own as well as the possibility of using **NAR-fa** as a beneficial property modifier of many other systems and thermosets and also being used as an initiator for polymerization at lower than usual temperature, makes this new resin an extremely promising and very attractive candidate for high performance and fire resistant polymeric and composite materials.

Finally, it is worth highlighting the greatness of simplicity. This case reflects the extremely simple but highly powerful synthetic strategy followed to synthesize the fully bio-based latent catalyst-containing benzoxazine resin exploiting a responsive hydrogen-bonding motif. This responsive bio-resin was used as an initiator and especially as a property modifier of other systems. The very easy ways of obtaining and using the bio-resin to form simple systems with greatly enhanced properties allow straightforwardly envisaging genuine real-life applications, minimizing costs and optimizing production times.

Conflicts of interest

The authors declare no competing financial interest.

Acknowledgements

The authors acknowledge the financial support from the National Natural Science Foundation of China (51603093), the Science and Technology Agency of Jiangsu Province (BK 20160515), and the China Postdoctoral Science Foundation (2018T110451). PF is a member of the Scientific and Technological Researcher Career at CONICET (Argentina).

Notes and references

1 N. V. Handa, S. Li, J. A. Gerbec, N. Sumitani, C. J. Hawker and D. Klinger, *J. Am. Chem. Soc.*, 2016, **138**, 6400–6403.
2 N. N. Ghosh, B. Kiskan and Y. Yagci, *Prog. Polym. Sci.*, 2007, **32**, 1344–1391.
3 X. Ning and H. Ishida, *J. Polym. Sci., Part A: Polym. Chem.*, 1994, **32**, 1121–1129.
4 H. Ishida and T. Agag, *Handbook of Benzoxazine Resins*, Elsevier, Amsterdam, 2011.
5 H. Ishida and P. Froimowicz, *Advanced and Emerging Polybenzoxazine Science and Technology*, Elsevier, Amsterdam, 2017.

6 H. Ishida and H. Y. Low, *Macromolecules*, 1997, **30**, 1099–1106.
7 K. Zhang and X. Yu, *Macromolecules*, 2018, **51**, 6524–6533.
8 L. Han, M. L. Salum, K. Zhang, P. Froimowicz and H. Ishida, *J. Polym. Sci., Part A: Polym. Chem.*, 2017, **55**, 3434–3445.
9 N. K. Sini and T. Endo, *Macromolecules*, 2016, **49**, 8466–8478.
10 Z. Deliballi, B. Kiskan and Y. Yagci, *Polym. Chem.*, 2018, **9**, 178–183.
11 K. Zhang, L. Han, P. Froimowicz and H. Ishida, *Macromolecules*, 2017, **50**, 6552–6560.
12 J. Wu, Y. Xi, G. T. McCandless, Y. Xie, R. Menon, Y. Patel, D. J. Yang, S. T. Iacono and B. M. Novak, *Macromolecules*, 2015, **48**, 6087–6095.
13 S. W. Kuo, Y. C. Wu, C. F. Wang and K. U. Jeong, *J. Phys. Chem. C*, 2009, **113**, 20666–20673.
14 C. F. Wang, Y. C. Su, S. W. Kuo, C. F. Huang, Y. C. Sheen and F. C. Chang, *Angew. Chem., Int. Ed.*, 2006, **45**, 2248–2251.
15 J. Sun, W. Wei, Y. Xu, J. Qu, X. Liu and T. Endo, *RSC Adv.*, 2015, **5**, 19048–19057.
16 G. Kaya, B. Kiskan and Y. Yagci, *Macromolecules*, 2018, **51**, 1688–1695.
17 S. Li and T. Zou, *J. Appl. Polym. Sci.*, 2012, **123**, 922–928.
18 C. Liu, D. Shen, R. M. Sebastián, J. Marquet and R. Schönfeld, *Polymer*, 2013, **54**, 2873–2878.
19 R. Kudoh, A. Sudo and T. Endo, *Macromolecules*, 2010, **43**, 1185–1187.
20 L. C. Hsuan, Y. R. Feng, K. H. Dai, H. C. Chang and T. Y. Juang, *J. Polym. Sci., Part A: Polym. Chem.*, 2013, **51**, 2686–2694.
21 C. J. Higginson, K. G. Malollari, Y. Xu, A. V. Kelleghan, N. G. Ricapito and P. B. Messersmith, *Angew. Chem., Int. Ed.*, 2019, **58**, 12271–12279.
22 K. Kudo, M. Furutani and K. Arimitsu, *ACS Macro Lett.*, 2015, **4**, 1085–1088.
23 W. Zhang, P. Froimowicz, C. R. Arza, S. Ohashi, Z. Xin and H. Ishida, *Macromolecules*, 2016, **49**, 7129–7140.
24 C. J. Moore, *Environ. Res.*, 2008, **108**, 131–139.
25 E. Calò, A. Maffezzoli, G. Mele, F. Martina, S. E. Mazzetto, A. Tarzia and C. Stifani, *Green Chem.*, 2007, **9**, 754–759.
26 P. Thirukumaran, A. S. Parveen and M. Sarojadevi, *ACS Sustainable Chem. Eng.*, 2014, **2**, 2790–2801.
27 C. Wang, J. Sun, X. Liu, A. Sudo and T. Endo, *Green Chem.*, 2012, **14**, 2799–2806.
28 P. Froimowicz, R. C. Arza, L. Han and H. Ishida, *ChemSusChem*, 2016, **9**, 1921–1928.
29 J. Dai, N. Teng, Y. Peng, Y. Liu, L. Cao, J. Zhu and X. Liu, *ChemSusChem*, 2018, **11**, 3175–3183.
30 K. Zhang, M. Han, Y. Liu and P. Froimowicz, *ACS Sustainable Chem. Eng.*, 2019, **7**, 9399–9407.
31 Y. Oh, K. M. Lee, D. Jung, J. A. Chae, H. J. Kim, M. Chang, J. J. Park and H. Kim, *ACS Macro Lett.*, 2019, **8**, 239–244.
32 N. Gel-Moreto, R. Streich and R. Galensa, *Electrophoresis*, 2003, **24**, 2716–2722.
33 H. Wang, M. G. Nair, G. M. Strasburg, A. M. Booren and J. I. Gray, *J. Agric. Food Chem.*, 1999, **47**, 840–844.
34 S. P. Teong, G. Yi and Y. Zhang, *Green Chem.*, 2014, **16**, 2015–2026.
35 P. Froimowicz, K. Zhang and H. Ishida, *Chem. – Eur. J.*, 2016, **22**, 2691–2707.
36 H. E. Kissinger, *Anal. Chem.*, 1957, **29**, 1702–1706.
37 T. Ozawa, *Polymer*, 1971, **12**, 150–158.
38 K. Zhang and H. Ishida, *Polym. Chem.*, 2015, **6**, 2541–2550.
39 M. Baqar, T. Agag, H. Ishida and S. Qutubuddin, *React. Funct. Polym.*, 2013, **73**, 360–368.
40 J. A. Dudek and J. A. Kargol, *Int. J. Thermophys.*, 1988, **9**, 245–253.
41 J. Wang, M. Q. Wu, W. B. Liu, S. W. Yang, J. W. Bai, Q. Q. Ding and Y. Li, *Eur. Polym. J.*, 2010, **46**, 1024–1031.
42 D. W. van Krevelen, *Polymer*, 1975, **16**, 615–620.
43 S. Mallakpour and V. Behranvand, *Colloid Polym. Sci.*, 2014, **293**, 333–339.
44 K. Zhang, Z. Shang, C. J. Evans, L. Han, H. Ishida and S. Yang, *Macromolecules*, 2018, **51**, 7574–7585.
45 T. Agag, J. Liu, R. Graf, H. W. Spiess and H. Ishida, *Macromolecules*, 2012, **45**, 8991–8997.
46 R. N. Walters and R. E. Lyon, *J. Appl. Polym. Sci.*, 2003, **87**, 548–563.